Using an inverse method to estimate the hydraulic properties of crusted soils from tension-disc infiltrometer data

Jiří Šimůnek [a,*], Rafael Angulo-Jaramillo [b], Marcel G. Schaap [a], Jean-Pierre Vandervaere [b], Martinus Th. van Genuchten [a]

[a] *U.S. Salinity Laboratory, USDA, ARS, 450 West Big Springs Road, Riverside, CA 92507-4617, USA*
[b] *Laboratoire d'étude des Transferts en Hydrologie et Environment (LTHE, CNRS URA 1512, INPG, UJF) BP 53, 38041 Grenoble Cedex 9, France*

Abstract

An inverse procedure was used to estimate the soil hydraulic characteristics of a two-layered soil system—soil surface crust and subsoil—from data obtained during a tension-disc infiltration experiment. The inverse procedure combined the Levenberg–Marquardt nonlinear parameter optimization method with a numerical solution of the axisymmetric variably-saturated flow equation. The objective function was defined in terms of the cumulative infiltration curve and the final water content measured directly below the tension-disc infiltrometer at the end of the experiment; this final water content was assumed to correspond to the final supply pressure head. We analyzed two infiltration experiments carried out with a 25-cm diameter tension-disc infiltrometer. One experiment was carried out on a two-layered system, and a second after removal of the surface crust covering the sandy subsoil. Both experiments were performed with six consecutive supply tensions. We first analyzed the infiltration experiment for the subsoil only, thus yielding its hydraulic characteristics. Subsequent analysis of the infiltration experiment for the two-layered system with known hydraulic properties of the subsoil provided estimates of the hydraulic properties of the surface crust. We further compared the estimated hydraulic parameters of the subsoil with those obtained using Wooding's analytical method [Wooding, R.A., 1968. Steady infiltration from a shallow circular pond. Water Resour. Res. 4, 1259–1273] and predictions based on a neural network model requiring textural input information. All three methods generated roughly the same results. The numerical inversion technique proved to be a convenient tool for

---

* Corresponding author. Tel: + 1-909-369-4865; Fax: + 1-909-342-4964; E-mail: jsimunek@ussl.ars.usda.gov

1. Introduction

A large number of measurements were carried out during the soil program part of the HAPEX (Hydrologic Atmospheric Pilot Experiment)-Sahel (climatic region bordering the southern Sahara from Senegal to Somalia) regional-scale experiment (Goutorbe et al., 1994; Cuenca et al., 1997). Soil-related measurements included neutron probe and TDR measurements of the profile soil water content, tensiometer measurements of the soil water potential, particle-size analyses, and infiltration rate measurements. The type of data collected and the experimental set-ups are documented by Cuenca et al. (1997) and Vandervaere et al. (1997), among others. The overall objective of the experiment was to improve the understanding of the physical processes of the Earth's ecosystem, the hydrologic system, and the atmospheric system (Cuenca et al., 1997).

An important feature affecting the water balance in many tropical and subtropical regions is the development of surface crusts in loamy and sandy soils (Casenave and Valentin, 1992; Valentin and Bresson, 1992). These crusts control the infiltration process and play a critical role in separating runoff and infiltrating water from the incoming rainfall. Valentin and Bresson (1992) classified surface crusts according to their formation, leading to three major classes: structural crusts, erosion crusts and depositional crusts, each with several subclasses. While structural crusts are formed by the impact of water drops, depositional crusts are formed by the translocation of fine particles and their deposition at a certain distance from their original location (Valentin and Bresson, 1992). Valentin and Bresson characterized erosion crusts as being rigid, thin and smooth surface layers enriched in fine particles, with the coarser particles removed by wind or overland flow. The surface crusts have usually a higher bulk density and smaller pores, and consequently a lower saturated conductivity than the underlying soil. Although the thickness of a surface crust is generally only a few millimeters, the small saturated hydraulic conductivity can significantly decrease the infiltration rate.

Several quasi-analytical solutions (Hillel and Gardner, 1969, 1970; Ahuja, 1974; Smilles et al., 1982) have been developed and used to calculate fluxes during steady and transient infiltration into a crusted soil profile from knowledge of the hydraulic properties of the crust and the underlying soil. These solutions are all for one-dimensional water flow. Because surface crusts are typically very thin, few field methods exist to estimate their hydraulic properties (Vandervaere et al., 1997). Vandervaere et al. (1997) recently proposed a method which uses

tension-disc (Perroux and White, 1988; Ankeny et al., 1991; Reynolds and Elrick, 1991; Logsdon et al., 1993, among many others) infiltration data at several water supply potentials, together with information from pre-installed mini-tensiometers below the soil crust to estimate the hydraulic conductivity, matric flux potential and sorptivity. Recent developments in transient flow theory (Haverkamp et al., 1994) were used for the analysis.

Another promising method for describing the soil crust/subsoil multi-layered system, and as an alternative to the traditional analysis of tension-disc infiltration experiments based on the analytical solution of Wooding (1968), assuming a homogeneous profile, is the use of parameter estimation using numerical inversion. Šimůnek and van Genuchten (1996, 1997) recently suggested a numerical inversion method to estimate the hydraulic properties from cumulative infiltration data obtained with a tension-disc permeameter at several consecutive tensions. Information required for a successful inversion, in addition to the cumulative infiltration with time, included information about the initial and final water contents before and after the infiltration experiment (Šimůnek and van Genuchten, 1997). Using numerically simulated data, they showed that the method can provide information on not only the hydraulic conductivity as is usually the case when invoking quasi-analytical methods, but also the soil water retention curve.

Soil hydraulic properties can also be estimated indirectly from correlations with basic soil data such as the sand, silt and clay fractions, bulk density and/or organic matter content. Such indirect methods, also called pedotransfer functions (PTFs), are often used to generate soil hydraulic properties in situations where measurements are too expensive, too cumbersome, or too difficult to carry out. Several PTFs predicting water retention and the saturated hydraulic conductivity, K_s, were tested on independent data by Tietje and Tapkenhinrichs (1993), Kern (1995), Williams et al. (1992), and Tietje and Hennings (1996). These studies show that many different types of PTFs exist in terms of input data, the predicted properties, mathematical structure and accuracy. Recently Pachepsky et al. (1996), Schaap and Bouten (1996) and Tamari et al. (1996) used neural network analyses to improve the PTF predictions. Schaap et al. (1998) showed that a hierarchical neural network system with increasing predictive capability could be obtained when more input variables were used for the estimation of the retention parameters of van Genuchten (1980) and K_s. They also showed that neural networks provided significantly better predictions than 10 previously published PTFs.

In this paper we will analyze two tension-disc infiltration experiments in order to estimate the soil hydraulic properties of a two-layered system involving a thin surface crust and the subsoil. We will first analyze the infiltration experiment carried out on the subsoil to obtain its hydraulic properties. This information is subsequently used to estimate the hydraulic properties of the surface crust by analyzing infiltration into the two-layered system. First, we will

use the method of Šimůnek and van Genuchten (1997) based on a numerical analysis of the field experiment. Results for the subsoil will be compared with those obtained with the classical steady-state analysis of Wooding (1968). Results will also be compared with soil hydraulic functions predicted from textural information using neural network analysis, as well as those given by Carsel and Parrish (1988) for a particular textural class. The neural network analysis will be applied only to the subsoil since no soil textural information was available for the very thin soil crust.

2. Experimental data

A large number of infiltration measurements with tension infiltrometers (Reynolds and Elrick, 1991; Ankeny et al., 1991; Thony et al., 1991) were taken as part of soil program of the HAPEX-Sahel regional-scale experiment during the summers of 1992 and 1993. The measurements were carried out at the Central Super Site East (Cuenca et al., 1997) using tension infiltrometers having disc diameters of 25, 8 and 4.85 cm. In this study we will analyze two experiments conducted on a fallow site with an erosion type crust using a 25-cm diameter disc. A thin (≈ 0.3 cm) layer of sand was placed between the disc membrane and the soil surface to improve hydraulic contact. Readings of the water supply tube were done visually. The soil was characterized according to the textural triangle of U.S. Department of Agriculture as a loamy sand with a particle size distribution given in Table 1. In one experiment (denoted as T2) the disc permeameter was placed directly on top of the soil surface (on the surface crust), while for a second experiment (denoted as T1) the crust was removed and the infiltrometer placed on the subsoil. The left-hand parts of Tables 2 and 3 summarize for the two experiments the applied supply pressure heads, h_0, the time intervals during which h_0 was applied (t_{init} is the starting time, and t_{final}

Table 1
Particle size distribution of the loamy sand

Particle diameter range (mm)	Percent by mass
0.000–0.002	11.2
0.002–0.020	1.9
0.020–0.050	2.5
0.050–0.100	12.0
0.100–0.200	26.6
0.200–0.500	37.7
0.500–1.000	7.3
1.000–2.000	0.8

Table 2
Wooding's analysis of experiment T1 (no crust)

h_0 [cm]	t_{init} [s]	t_{final} [s]	$Q(h_0)$ [ml s^{-1}]	h_a [cm]	$K(h_a)$ [cm s^{-1}]	α^* [cm^{-1}]	K_s [cm s^{-1}]
−11.5	0	2250	1.275				
−9.0	2430	333	1.564	−10.25	0.00128	0.0818	0.00296
−6.0	3510	4290	1.833	−7.5	0.00118	0.0530	0.00176
−3.0	4470	5115	2.224	−4.5	0.00159	0.0644	0.00213
−1.0	5295	5835	2.608	−2.0	0.00216	0.0798	0.00253
−0.1	6015	6450	3.233	−0.55	0.00416	0.2384	0.00473

the final time) and the final ('steady-state') infiltration rates, $Q(h_0)$, for a particular supply pressure head. Tables 2 and 3 also give results of Wooding's analysis (to be discussed later).

Disturbed gravimetric samples were taken at two depths before and after the infiltration experiments to determine the initial and final water contents. Undisturbed samples were also collected to obtain the dry bulk density needed to convert gravimetric water contents into volumetric values. The bulk density was found to be highest for the top soil (1.794 g cm^{-3} for the soil layer to 7.5 cm) and gradually decreased with depth (1.632 g cm^{-3} at a depth of 17.5 cm). The initial water contents in the surface layer for experiments T1 and T2 were 0.149 and 0.0369 cm^3 cm^{-3}, respectively, and the final water contents below the tension-disc infiltrometer at the end of the infiltration experiments 0.275 and 0.232, respectively.

3. Data analysis

The tension infiltrometer data will be analyzed in two ways. One method uses a numerical solution of the variably-saturated water flow equation (Šimůnek et

Table 3
Wooding's analysis of experiment T2 (with crust)

h_0 [cm]	t_{init} [s]	t_{final} [s]	$Q(h_0)$ [ml s^{-1}]	h_a [cm]	$K(h_a)$ [cm s^{-1}]	α^* [cm^{-1}]	K_s [cm s^{-1}]
−10.0	0	1740	0.0639				
−7.0	2040	2940	0.0643	−8.5	0.223×10^{-5}	0.00177	0.226×10^{-5}
−5.0	3240	4080	0.0652	−6.0	0.912×10^{-5}	0.00757	0.955×10^{-5}
−3.0	4390	5220	0.0694	−4.0	0.316×10^{-4}	0.03054	0.357×10^{-4}
−1.0	5520	7020	0.0676	−2.0	-0.204×10^{-4}	−0.0130	-0.199×10^{-4}
−0.5	7320	8115	0.0677	−0.75	0.236×10^{-5}	0.0177	0.236×10^{-5}

al., 1996) coupled with the minimization method of Marquardt–Levenberg (Marquardt, 1963). The objective function being minimized will be defined in terms of cumulative infiltration data and the final water content at the end of the infiltration experiment, while the initial condition is given in terms of the water content (Šimůnek and van Genuchten, 1997). The final water content below the tension-disc infiltrometer, θ_f, is assumed to correspond to the final supply pressure head at the end of the experiment. The data will be analysed also using the analytical solution of Wooding (1968) to the final ('steady-state') infiltration fluxes at particular supply pressure heads. The soil hydraulic parameters of the subsoil will also be estimated by neural network prediction from textural information (Schaap et al., 1998).

3.1. Numerical model

The governing flow equation for radially symmetric isothermal Darcian flow in a variably-saturated isotropic rigid porous medium is given by the following modified form of the Richards' equation (Warrick, 1992):

$$\frac{\partial \theta}{\partial t} = \frac{1}{r} \frac{\partial}{\partial r}\left(rK \frac{\partial h}{\partial r} \right) + \frac{\partial}{\partial z}\left(K \frac{\partial h}{\partial z} \right) + \frac{\partial K}{\partial z} \tag{1}$$

where θ is the volumetric water content [$L^3 \, L^{-3}$], h is the pressure head [L], K is the hydraulic conductivity [$L \, T^{-1}$], r is a radial coordinate [L], z is a vertical coordinate [L] positive upward, and t is time [T]. Note that we assume in Eq. (1) that the porous medium is isotropic, although not necessary homogeneous. Initial and boundary equations applicable to a disc-tension infiltrometer experiment (Warrick, 1992) are as follows:

$$\theta(r,z,t) = \theta_i(z) \qquad t = 0 \tag{2}$$

$$h(r,z,t) = h_0(t) \qquad 0 < r < r_0, \; z = 0 \tag{3}$$

$$-\frac{\partial h(r,z,t)}{\partial z} - 1 = 0 \qquad r > r_0, \; z = 0 \tag{4}$$

$$\theta(r,z,t) = \theta_i(z) \qquad r^2 + z^2 \to \infty \tag{5}$$

where θ_i is the initial water content [$L^3 \, L^{-3}$], $h_0(t)$ is the time-variable supply pressure head imposed by the tension-disc infiltrometer [L] and r_0 is the disc radius [L]. Note that the initial condition is given in terms of the water content. Šimůnek and van Genuchten (1997) showed that having this initial condition, as compared to using the pressure head, insures a more stable and unique solution of the inverse problem. Soil surface boundary conditions below the disc permeameter and the remaining soil surface are represented by Eqs. (3) and (4), respectively. Eq. (5) assumes that all subsurface boundaries are so far removed

from the supply source that they are not affected during the infiltration experiment. Eq. (1), subject to the above initial and boundary conditions, was solved numerically using a quasi-three-dimensional (axisymmetric) finite element code HYDRUS-2D as documented by Šimůnek et al. (1996).

3.2. Soil hydraulic properties

A model of the unsaturated soil hydraulic properties must be selected prior to application of the numerical solution of the Richards' equation. Most analytical solutions for infiltration are based on the exponential function of Gardner (1958), which describes the dependence of the unsaturated hydraulic conductivity on the pressure head. This function, however, was found to be the least successful (Leij et al., 1997) of five different functions studied in terms describing observed hydraulic conductivity data taken from the UNSODA unsaturated soil hydraulic database (Leij et al., 1996). In our analysis we will use the unsaturated soil hydraulic functions of van Genuchten (1980) which performed better. These functions are given by

$$S_e(h) = \frac{\theta(h) - \theta_r}{\theta_s - \theta_r} = \frac{1}{\left(1 + |\alpha h|^n\right)^m} \qquad h < 0$$

$$\theta(h) = \theta_s \qquad\qquad\qquad h \geq 0 \tag{6}$$

$$K(\theta) = K_s S_e^l \left[1 - \left(1 - S_e^{1/m}\right)^m\right]^2 \qquad h < 0$$

$$K(\theta) = K_s \qquad\qquad\qquad h \geq 0 \tag{7}$$

where S_e is the effective water content $[-]$, K_s is the saturated hydraulic conductivity $[L\ T^{-1}]$, θ_r and θ_s denote the residual and saturated water contents $[L^3\ L^{-3}]$, respectively; l is a pore-connectivity parameter $[-]$, and $\alpha\ [L^{-1}]$ and $n\ [-]$ and $m\ (= 1 - 1/n)\ [-]$ are empirical parameters. The pore-connectivity parameter l in the hydraulic conductivity function was estimated by Mualem (1976) to be 0.5 as an average for many soils. Assuming $l = 0.5$, the hydraulic characteristics defined by Eqs. (6) and (7) contain five unknown parameters: θ_r, θ_s, α, n, and K_s. Since saturation will never be reached during a tension infiltration experiment, K_s and θ_s in this study are interpreted as being extrapolated, empirical parameters outside the range of the disc experiment (Šimůnek and van Genuchten, 1996). Also, tension-disc infiltration in general is a wetting process (assuming that one can neglect internal drainage at the initial pressure head and during short periods when the infiltration process is interrupted in order to refill the water supply tube); this means that the hydraulic parameters in Eqs. (6) and (7) represent wetting branches of the unsaturated hydraulic properties.

3.3. Inverse solution

The objective function Φ to be minimized during the parameter estimation process can be formulated using either cumulative infiltration data only, or cumulative infiltration data in combination with additional information such as the observed water content corresponding to the final supply pressure head, or transient pressure head and/or water content measurements within the soil profile. The objective function for multiple measurement sets is defined as (Šimůnek and van Genuchten, 1996)

$$\Phi(\boldsymbol{\beta}, q_1, \ldots, q_m) = \sum_{j=1}^{m} \left(v_j \sum_{j=1}^{n_j} w_{ij} \left[q_j * (t_i) - q_j(t_i, \beta) \right]^2 \right) \tag{8}$$

where m represents the different sets of measurements such as the cumulative infiltration data (I) and the final water content (θ_f), n_j is the number of measurements in a particular set, $q_j * (t_i)$ are specific measurements at time t_i for the jth measurement set, $\boldsymbol{\beta}$ is the vector of optimized parameters (e.g., θ_r, θ_s, α, n, and K_s), $q_j(t_i, \boldsymbol{\beta})$ are the corresponding model predictions for the parameter vector $\boldsymbol{\beta}$, and v_j and $w_{i,j}$ are weights associated with a particular measurement set or point, respectively. We assume for now that the weighting coefficients $w_{i,j}$ in Eq. (8) are equal to one, that is, the variances of the errors inside a particular measurement set are assumed the same. The weighting coefficients v_j, which minimize differences in weighting between different data types because of different absolute values and numbers of data involved, are given by (Clausnitzer and Hopmans, 1995)

$$v_j = \frac{1}{n_j \sigma_j^2} \tag{9}$$

thus defining the objective function as the average weighted squared deviation normalized by measurement variances σ_j^2. Since the final water content is only one number and its variance can not be defined, the weight for this data point is assumed to be one.

Minimization of the objective function Φ is accomplished by using the Levenberg–Marquardt nonlinear minimization method (Marquardt, 1963). This method was found to be very effective and has become a standard in nonlinear least-square fitting among soil scientists and hydrologists (van Genuchten, 1981; Kool et al., 1985, 1987).

3.4. Wooding's analytical solution

The variably-saturated water flow equation can be solved analytically for infiltration from a circular source with a constant pressure head at the soil

surface and with the unsaturated hydraulic conductivity described by the exponential model of Gardner (1958)

$$K(h) = K_s \exp(\alpha^* h) \tag{10}$$

The analytical solution was derived by Wooding (1968) and is given by

$$Q(h_0) = \left(\pi r_0^2 + \frac{4r_0}{\alpha^*} \right) K(h_0) \tag{11}$$

where Q is the steady-state infiltration rate [$L^3 T^{-1}$], r_0 is the radius of the disc [L], h_0 is the wetting pressure head [L], $K(h_0)$ is the unsaturated hydraulic conductivity [$L T^{-1}$] at pressure head h_0, and α^* is the sorptive number (White and Sully, 1987). The first term on the right represents the effect of gravitational forces and the second term the effect of capillary forces. Wooding's analytical solution has two unknown variables, i.e., the hydraulic conductivity $K(h_0)$ (or the saturated hydraulic conductivity K_s after using Gardner's equation) and the sorptive number α^*. The traditional analysis of tension-disc experiments using the solution of Wooding (1968) hence requires two steady-state fluxes obtained with the same disc infiltrometer at different tensions (Ankeny et al., 1991), or with two infiltrometers of different diameters at the same tension (Smettem and Clothier, 1989). We note here that Wooding's analytical solution assumes that the soil is homogeneous, isotropic, and has a uniform initial water content. When these restrictive assumptions are not fulfilled, Wooding's analysis often leads to negative values of K_s (Hussen and Warrick, 1993; Logsdon and Jaynes, 1993; Vandervaere et al., 1997).

The theory for obtaining the unsaturated hydraulic conductivity in the middle of an interval between two successively applied pressure heads was described previously by Ankeny et al. (1991), Reynolds and Elrick (1991) and Jarvis and Messing (1995), among others. The approach assumes that the sorptive number α^* in Gardner's exponential model is constant over the interval between two adjacent supply pressure heads such that

$$\alpha^*_{i+1/2} = \frac{\ln \dfrac{Q_i}{Q_{i+1}}}{h_i - h_{i+1}} \qquad i = 1, \ldots, n-1 \tag{12}$$

where n is the number of infiltration tensions used, and where the subscript $1/2$ on α^* indicates estimation in the middle of two adjacent supply pressure heads: $h_{i+1/2} = (h_i + h_{i+1})/2$. The unsaturated hydraulic conductivity at pressure head $h_{i+1/2}$ is then calculated as

$$K_{i+1/2} = \frac{Q_{i+1/2}}{\pi r_0^2 + \dfrac{4r_0}{\alpha^*_{i+1/2}}} \qquad i = 1, \ldots, n-1 \tag{13}$$

in which the estimated infiltration rate $Q_{i+1/2}$ in the middle ($h_{i+1/2}$) between two adjacent supply pressure heads is calculated as a geometric mean of the actual infiltration rates Q_i and Q_{i+1}:

$$Q_{i+1/2} = \exp\frac{\ln Q_i + \ln Q_{i+1}}{2} \qquad i = 1,\ldots,n-1 \tag{14}$$

The saturated hydraulic conductivity K_s can be calculated from Eq. (10) using known values of $h_{i+1/2}$, $K_{i+1/2}$ and $\alpha^*_{i+1/2}$ as follows

$$K_s = \frac{K_{i+1/2}}{\exp\left(\alpha^*_{i+1/2}\, h_{i+1/2}\right)} \tag{15}$$

4. Results and discussion

We first analyze experiment T1 for the case without a surface crust. The flow domain for the numerical solution was discretized into 722 triangular elements and 200 nodes, with a relatively fine grid close to the soil surface and below the disc, and larger elements farther away from the disc. Limiting the number of elements is important to avoid excessive CPU times since the direct numerical solution has to be carried out many times during the parameter optimization process. The adopted discretization was thought to be a good compromise between solution precision and required computer time. The relatively coarse discretization scheme resulted in mass balance errors which were always smaller than 0.1%.

Fig. 1 shows the measured and calculated cumulative infiltration curves, as well as their differences, for experiment T1 (no crust) when the objective function, $\Phi(\boldsymbol{\beta}, I, \theta_f)$, was defined in terms of the cumulative infiltration, I, and the water content, θ_f, corresponding to the final pressure head. The latter information was included as a point on the retention curve, i.e., $\theta(h) = 0.275(-0.1$ cm$)$. The soil profile was considered homogenous with an initial water content of 0.149. Notice the small breaks in the cumulative infiltration curve (Fig. 1a) caused by momentary removal of the infiltrometer from the soil surface while resupplying it with water and adjusting the tension for a new time interval (t_{final}, t_{init}) (see Tables 2 and 3). The interruptions in infiltration took about 3 and 5 min for experiments T1 and T2, respectively. More than 10.5 l of water infiltrated during experiment T1. The supply tubes could not hold this much water and water hence had to be resupplied during the runs. The interruptions, however, did not cause any problem for the numerical solution since during these times the Dirichlet boundary condition below the disc permeameter could be simply replaced by a zero-flux Neumann type boundary condition. Notice the very close agreement between the measured and optimized cumulative infiltration curves (Fig. 1b); the largest deviations were generally less than 60 ml, being only about 0.5% of the total infiltration volume.
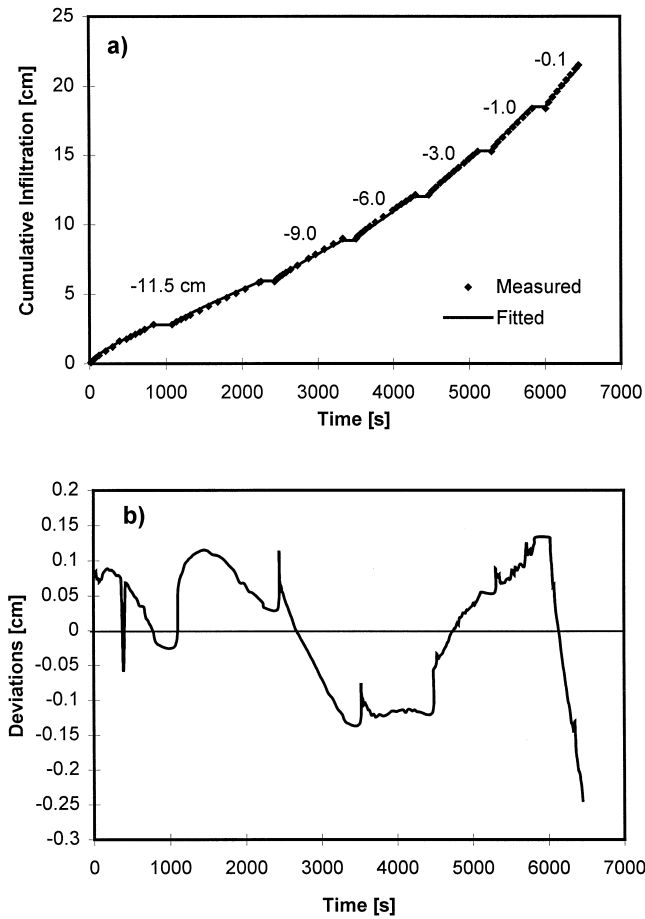
Fig. 1. Experiment T1: measured and optimized cumulative infiltration curves (a) and their differences (b) for the soil profile without the surface crust.

Since nearly all optimizations initially gave θ_r estimates equal to or very close to zero, we decided to fix θ_r to zero for all cases. Van Genuchten's hydraulic parameters obtained by numerical inversion, together with the final value of the objective function Φ_f, are given in Table 4. Notice the relatively high precision of the final parameter estimates as judged from the normalized standard deviation of the parameter estimate, NSD [%] given by

$$\text{NSD} = 100 \frac{\sigma}{\beta_j} \tag{16}$$

where σ is the standard deviation of the parameter estimate, calculated from knowledge of the objective function, the number of observations, the number of unknown fitted parameters, and an inverse matrix (van Genuchten et al., 1991). The narrow confidence interval for θ_s reflects the large weight given to the final

Table 4
Soil hydraulic parameters for loamy sand subsoil

Parameters	Numerical inversion				Neural network prediction		Value from Carsel and Parrish (1988)
	$\Phi(\boldsymbol{\beta},I,\theta_{\mathrm{f}})$		$\Phi(\boldsymbol{\beta},I,\theta_{\mathrm{p}})$				
	Value	NSD [%]	Value	NSD [%]	Value	NSD [%]	
θ_{r}	0.0	–	0.0	–	0.0528	23.8	0.057
θ_{s}	0.275	0.03	0.296	0.04	0.3266	4.35	0.41
α [cm^{-1}]	0.0303	2.70	0.0306	0.95	0.0219	26.9	0.124
n	1.91	3.49	2.016	2.21	1.6527	7.42	2.28
K_{s} [cm s^{-1}]	0.00221	4.08	0.00209	2.9	0.000416	25.1	0.00405
Φ_{f}	0.000187		0.000235				

water content in the optimization. Table 5 shows the correlation matrix for the optimized parameters. The saturated water content, θ_s, was uncorrelated with any other optimized parameters. However, a high negative correlation exists between K_s and n. This correlation reflects the shape of the objective function which shows a hyperbolical valley in the parameter plane K_s and n (see figure 6 in Šimůnek and van Genuchten, 1997). Nevertheless, even these two parameters were estimated with a relatively high level of confidence (Table 4).

The saturated water content, θ_s, estimated by numerical inversion was equal to 0.275 which is about 0.045 less than the porosity as calculated from the bulk density. This result is consistent with observations (e.g., Klute, 1986; Baumer, 1992) that field-measured θ_s-values are generally about 10–20% lower than the porosity. Also contributing to the observed difference in this case is likely the high permeability of the loamy sand subsoil (K_s was nearly 200 cm d^{-1}). The high value of K_s may have caused already significant drainage and redistribution of water in the soil profile during the approximately 60 s it took after completion of the infiltration experiment to remove the tension disc and collect the soil samples for laboratory determination of the water content. Hence, the collected samples may not have corresponded exactly with the final supply pressure head.

To further study this redistribution problem we repeated the numerical inversion with a modified objective function $\Phi(\boldsymbol{\beta}, I, \theta_p)$ which included the final water content not as a fixed point of the retention curve, but as a transient value of the water content, θ_p, below the disc measured 60 s after the end of the infiltration experiment. This approach permits the numerical model to calculate the amount of water draining from the upper soil profile before actual sampling took place. The results of this numerical inversion are also presented in Table 4. The objective function has now a somewhat higher, but not significantly different value. The estimated θ_s was slightly higher (0.296) than in the previous case, being now only about 0.025 lower than the porosity. Values of the other optimized parameters are about the same. The correlation matrix (not further presented here) also had a similar structure.

The measured cumulative infiltration curve was also analyzed using Wooding's analytical solution as given by Eqs. (10) through (15). Wooding's analysis requires steady-state fluxes; if steady-state is not reached the soil hydraulic

Table 5
Correlation matrix for optimized parameters for experiment T1

Parameter	α	n	θ_s	K_s
α	1.0			
n	0.899	1.0		
θ_s	0.032	0.013	1.0	
K_s	-0.813	-0.986	-0.009	1.0

conductivities will be somewhat under- or over-estimated. The minimum time required for the infiltration rate to approach steady-state depends on soil texture, the size of the infiltration disc and the supply pressure head. The steady-state infiltration rate is reached relatively fast for coarse-textured soils, as in our case. The time, t_{grav}, after which gravitational forces dominate capillary effects can be calculated from knowledge of the sorptivity and the conductivity as follows (Philip, 1969):

$$t_{grav} = \left(\frac{S}{K} \right)^2 \tag{17}$$

where S is sorptivity [$LT^{-0.5}$]. From values given in Vandervaere et al. (1997) and from our estimates of the hydraulic conductivity, we calculated that t_{grav} is approximately equal to 4 and 22 min for supply tensions of 1 and 10 cm, respectively. The time intervals used for our supply tensions were in most cases larger than t_{grav}.

We obtained the final infiltration rates for particular supply pressure heads by determining the slope of the cumulative infiltration curve (Fig. 1a) using linear regression analysis on the last six measured values. The results of Wooding's analysis are summarized in Table 2. This table gives unsaturated hydraulic conductivities $K(h_a)$ corresponding to the middle of the pressure head interval, h_a, between two consecutive supply pressure heads, the sorptive number α^*, and the saturated hydraulic conductivity, K_s, as extrapolated from $K(h_a)$ using the estimated α^*. All calculated K_s-values were of the same order, except when estimated from the highest supply pressure head interval in which case K_s was about twice as high. Also, α^* for this pressure head interval was about three times the other values.

Fig. 2 compares the unsaturated hydraulic conductivity function as obtained with the numerical parameter estimation method with local values of the hydraulic conductivity obtained for pressure heads in the middle of two supply tensions using the Wooding's analysis (Table 2). Both methods gave almost identical results for pressure heads in the interval between -2 and -10.25 cm. The value of the hydraulic conductivity for the highest pressure head interval was overestimated by a factor of two using Wooding's analysis. Fig. 2 shows that when the underlying assumptions of the two methods are satisfied (i.e., approximate homogeneity of the soil profile and steady-state flux for analytical method), both methods provide approximately the same results.

Table 4 gives, in addition to van Genuchten's parameters obtained by numerical inversion, the hydraulic parameters obtained with a neural network prediction from the measured soil texture classes and bulk density, and the average parameter values for the loamy sand soil textural group as estimated by Carsel and Parrish (1988) from an analysis of a large number of soils. We used two neural network models derived by Schaap et al. (1998) to predict the retention parameters of Eq. (6), as well as K_s, from sand, silt and clay
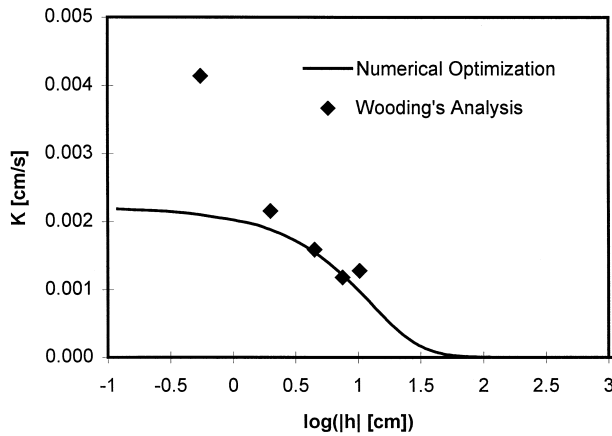
Fig. 2. Unsaturated hydraulic conductivities of the subsoil calculated using Wooding's analytical solution for particular pressure heads and using the numerical inversion.

percentages (derived from Table 1) and the subsoil bulk density. The three-layer back-propagation neural networks were calibrated and validated on a large soil database consisting of 1209 samples from the USA (Rawls, personal communication). The variation of textural, bulk density and hydraulic data in this database makes the calibrated neural network widely applicable. Validation results showed that the neural networks performed better than traditional regression equations. Water retention and saturated hydraulic conductivities were predicted with an average accuracy of, respectively, 0.087 cm^3 cm^{-3} and 0.53 log(cm d^{-1}) over the entire data set (Schaap et al., 1998).

Fig. 3 shows both the retention and the hydraulic conductivity functions for the parameters in Table 4. Notice the relatively good agreement between the hydraulic properties obtained by numerical inversion and the neural network prediction. The entire retention curve obtained by numerical inversion using objective function $\Phi(\boldsymbol{\beta}, I, \theta_f)$ was shifted by about 0.05 cm^3 cm^{-3} downwards as compared to the neural network prediction, whereas the water content interval between θ_s and θ_r was about the same (equal to 0.27). The initial condition for experiment T2 was 0.036 which is lower than θ_r predicted with the neural network; this result explains the fact that our numerical inversion gave a smaller value of θ_r. The neural network model predicted θ_s to be more or less equal to the porosity. The values of α predicted by numerical inversion and the neural network were about the same, as was the case with n. However, K_s predicted with the neural network was about five times lower than K_s predicted by numerical inversion. The value of n obtained by numerical inversion was similar to the average n of the loamy sand soil textural group as given by Carsel and Parrish (1988). The highest difference between parameters obtained with numerical inversion and average parameters of the loamy sand textural group were for α. Parameters for textural groups as derived by Carsel and Parrish
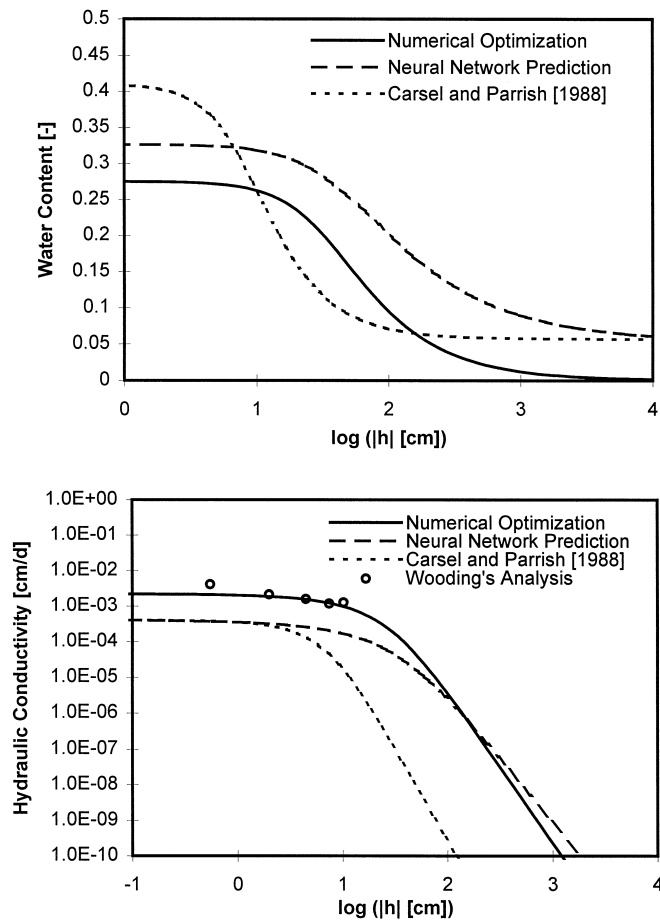
Fig. 3. Soil hydraulic functions obtained with numerical inversion for experiment T1, using neural network prediction for data from Table 1, using Wooding's analysis, and for loamy sand textural group (Carsel and Parrish, 1988).

(1988) represent an entire soil class, and hence some differences should be expected. Neural network predictions of the soil hydraulic parameters, on the other hand, provide parameter values for a specific soil, and hence should yield better agreement.

In the second step we analyzed experiment T2 when the tension permeameter was placed directly on the soil surface. The cumulative infiltration data were again analyzed by numerical inversion and using Wooding's method. We stress here that the assumptions of Wooding's solution were not fulfilled since the soil profile was not homogeneous but consisted of two layers, a crust and the subsoil. This complication, however, is not an issue for the numerical solution which readily accommodates multi-layered profiles. The soil profile was assumed to consist of a 0.5 cm thick top layer representing the surface crust

(erosion crusts are in general only about 0.1 cm thick (Casenave and Valentin, 1992); we used 0.5 cm for numerical reasons), and the underlying subsoil where hydraulic parameters were assumed known from the earlier analysis involving the subsoil only (experiment T1 in Table 4). Hence, only the parameters of the surface layer were now assumed unknown and sought by numerical inversion. The optimized parameters are given in Table 6. The results indicate much lower confidence in the estimated parameter values for the surface crust as compared to parameters for subsoil (Table 4).

The measured and optimized cumulative infiltration curves, and their differences, are shown in Fig. 4. The maximum deviations were slightly higher than for experiment T1, about 2.5% of the cumulative infiltration volume. Notice that, as compared with experiment T1, a much smaller volume of water infiltrated. The lower infiltrated volume caused the saturated hydraulic conductivity K_s of the surface crust to be two orders of magnitude lower than for the subsoil. Also the water content interval between θ_s and θ_r was now only about 0.24. This result corresponds well with observations of Valentin and Bresson (1992) and Casenave and Valentin (1992) that the porosity of an erosion crust is generally very low. Casenave and Valentin (1992) estimated the infiltration rate into erosion-type surface crusts to be between 0.0 to 4.8 cm d^{-1}, with our estimated value (0.15 cm d^{-1}) being in this interval. The value of n was more characteristic for a clay loam textural group, while α and K_s were typical of a silty clay (Carsel and Parrish, 1988).

Table 3 presents results of Wooding's analysis for experiment T2. Note that the 'steady-state' infiltration rates increased, as expected, when the supply tension decreased to 3 cm. After that the infiltration rates actually decreased slightly. This result likely means that the air-entry value was reached at a pressure head of about -3 cm. For infiltration at lower tensions, the hydraulic conductivity remains then equal to K_s and only changes in the pressure head gradient can influence the infiltration rate. The resulting values for both K_s and α^* fluctuated several orders of magnitude between the different tension intervals, may be due to the underlying assumptions necessary for correct application of the Wooding's solution. In one case K_s even reached a negative value,

Table 6
Soil hydraulic parameters for surface crust

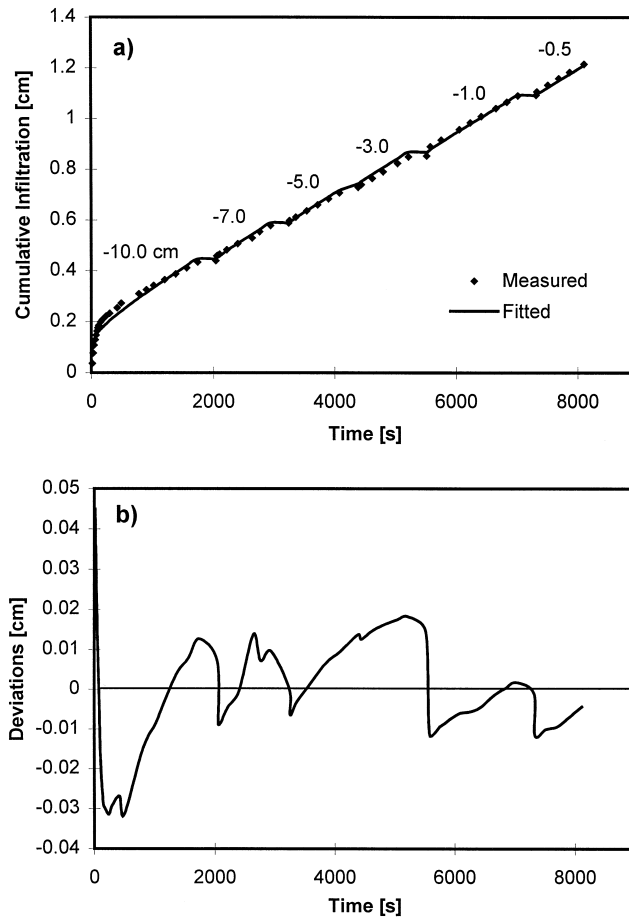| Parameters	Value	NSD [%]
θ_r	0.0	–
θ_s	0.245	2.51
α [cm^{-1}]	0.000411	11.4
n	1.35	8.98
K_s [cm s^{-1}]	0.0000017	27.1
Φ_f	0.00227	

Fig. 4. Experiment T2: measured and calculated cumulative infiltration curves (a) and their differences (b) for the soil profile with the surface crust.

further reflecting that Wooding's analysis is inappropriate for a two-layered soil profile.

5. Conclusions

We analyzed cumulative infiltration data from tension-disc infiltrometer by numerical inversion (Šimůnek and van Genuchten, 1997) and using the analytical solution of Wooding (1968). We first analyzed the infiltration experiment carried out on the subsoil only, from which we obtained its soil hydraulic characteristics. We subsequently analyzed the infiltration experiment for a two-layered system—crust and subsoil—with the assumption that the hydraulic characteristics of the subsoil are known from the previous analysis, thus leading to estimates of the hydraulic parameters of the surface crust. The hydraulic

parameters for the subsoil obtained by parameter estimation and Wooding's analytical method compared well with each other, and also with parameters obtained by means of a neural network prediction (Schaap et al., 1998) based on available soil textural information.

The numerical inversion technique allowed us to obtain the soil hydraulic properties of both the surface crust and the subsoil. Since direct measurements of the soil hydraulic properties of the surface crust are extremely difficult to obtain, no information was available for direct comparison with our numerical results. The saturated hydraulic conductivity K_s of the surface crust was found to be two orders of magnitude lower than for the subsoil.

While many laboratory and field methods exist (Klute, 1986) to determine the soil water retention and unsaturated hydraulic conductivity curves, most methods remain relatively expensive and too cumbersome for applications at relatively larger scales. Parameter estimation techniques provide an attractive alternative to more traditional, time consuming steady state methods which often are also limited to a relatively narrow range in the water content. Time-savings are possible since transient flow experiments generally cover a much broader range of water contents, while no need exists to reach flow equilibrium. The savings in time, however, are sometimes accompanied by a loss of accuracy since not all transient experiments will provide enough information to guarantee a unique solution (Šimůnek and van Genuchten, 1997). To avoid or limit such a loss of accuracy, detailed analyses should be carried out before a particular transient flow experiment is used to estimate the soil hydraulic properties (e.g., Toorman et al., 1992). An even faster and economical way of estimating the soil hydraulic parameters would be to use indirect methods, such as regression or neural network analyses, which relate the hydraulic parameters to more easily measured soil taxonomic data such as texture and bulk density (Schaap et al., 1998). The additional savings in cost and time of indirect methods are generally offset by an even larger loss of prediction accuracy (see Table 4).

References

Ankeny, M.D., Ahmed, M., Kaspar, T.C., Horton, R., 1991. Simple field method for determining unsaturated hydraulic conductivity. Soil Sci. Soc. Am. J. 55, 467–470.

Ahuja, L.R., 1974. Applicability of the Green–Ampt approach to water infiltration through surface crust. Soil Sci. 118, 283–288.

Baumer, O.W., 1992. Predicting unsaturated hydraulic parameters. In: van Genuchten, M.Th., Leij, F.J., Lund, L.J. (Eds.), Indirect Methods for Estimating the Hydraulic Properties of Unsaturated Soils. Proceedings of the International Workshop, Univ. California, Riverside, CA, pp. 341–354.

Carsel, R.F., Parrish, R.S., 1988. Developing joint probability distributions of soil water retention characteristics. Water Resour. Res. 24, 755–769.

Casenave, A., Valentin, C., 1992. A runoff capability classification system based on surface features criteria in semi-arid areas of West Africa. J. Hydrol. 130, 231–249.

Clausnitzer, V., Hopmans, J.W., 1995. Non-linear parameter estimation: LM_OPT. General-purpose optimization code based on the Levenberg–Marquardt algorithm. Land, Air and Water Resources Paper No. 100032, University of California, Davis, CA.

Cuenca, R.H., Brouwer, J., Chanzy, A., Droogers, P., Galle, S., Gaze, S.R., Sicot, M., Stricker, H., Angulo-Jaramillo, R., Boyle, S.A., Bromly, J., Chebhouni, A.G., Cooper, J.D., Dixon, A.J., Fies, J.-C., Gandah, M., Gaudu, J.-C., Laguerre, L., Soet, M., Steward, H.J., Vandervaere, J.-P., Vauclin, M., 1997. Soil measurements during HAPEX-Sahel intensive observation period. J. Hydrol. 188–189, 224–266.

Gardner, W.R., 1958. Some steady-state solutions of the unsaturated moisture flow equation with application to evaporation from a water table. Soil Sci. 85, 228–232.

Goutorbe, J.-P., Lebel, T., Tinga, A., Bessemoulin, P., Brouwer, J., Dolman, A.J., Engman, E.T., Gash, J.H.C., Hoepffner, M., Kabat, P., Monteny, B.A., Prince, S., Said, F., Sellers, P., Wallace, J.S., 1994. HAPEX-Sahel: a large scale study of land–atmosphere interactions in the semi-arid tropics. Ann. Geophys. 12, 53–64.

Haverkamp, R., Ross, P.J., Smettem, K.R.J., Parlange, J.Y., 1994. Three-dimensional analysis of infiltration from the disc infiltrometer: 2. Physically based infiltration equation. Water Resour. Res. 30, 2931–2935.

Hillel, D., Gardner, W.R., 1969. Steady infiltration into crust-topped profiles. Soil Sci. 108, 137–142.

Hillel, D., Gardner, W.R., 1970. Transient infiltration into crust-topped profiles. Soil Sci. 109, 69–74.

Hussen, A.A., Warrick, A.W., 1993. Alternative analysis of hydraulic data from the disc tension infiltrometers. Water Resour. Res. 29, 4103–4108.

Jarvis, N.J., Messing, I., 1995. Near-saturated hydraulic conductivity in soils of contrasting texture measured by tension infiltrometers. Soil Sci. Soc. Am. J. 59, 27–34.

Kern, J.S., 1995. Evaluation of soil water retention models based on basic soil physical properties. Soil Sci. Soc. Am. J. 59, 1134–1141.

Klute, A., 1986. Water retention: laboratory methods. In: Klute, A. (Ed.), Methods of Soil Analysis, Part 1—Physical and Mineralogical Methods, 2nd edn. Agronomy Monograph 9, pp. 635–662.

Kool, J.B., Parker, J.C., van Genuchten, M.Th., 1985. Determining soil hydraulic properties from one-step outflow experiments by parameter estimation: I. Theory and numerical studies. Soil Sci. Soc. Am. J. 49, 1348–1354.

Kool, J.B., Parker, J.C., van Genuchten, M.Th., 1987. Parameter estimation for unsaturated flow and transport models—a review. J. Hydrol. 91, 255–293.

Leij, F.J., Alves, W.J., van Genuchten, M.Th., 1996. The UNSODA unsaturated soil hydraulic database. EPA, Ada, OK.

Leij, F.J., Russell, W.B., Lesch, S.M., 1997. Closed-form expressions for water retention and conductivity data. Ground Water 35 (5), 848–858.

Logsdon, S.D., Jaynes, D.B., 1993. Methodology for determining hydraulic conductivity with tension infiltrometers. Soil Sci. Soc. Am. J. 57, 1426–1431.

Logsdon, S.D., McCoy, E.L., Allmaras, R.R., Linden, D.R., 1993. Macropore characterization by indirect methods. Soil Sci. 155, 316–324.

Marquardt, D.W., 1963. An algorithm for least-squares estimation of nonlinear parameters. SIAM J. Appl. Math. 11, 431–441.

Mualem, Y., 1976. A new model for predicting the hydraulic conductivity of unsaturated porous media. Water Resour. Res. 12, 513–522.

Pachepsky, Y.A., Timlin, D., Varallyay, G., 1996. Artificial neural networks to estimate soil water retention from easily measurable data. Soil Sci. Soc. Am. J. 60, 727–733.

Perroux, K.M., White, I., 1988. Design for disc permeameters. Soil Sci. Soc. Am. J. 52, 1205–1215.

Philip, J.R., 1969. Theory of infiltration. Adv. Hydrosci. 5, 215–296.

Reynolds, W.D., Elrick, D.E., 1991. Determination of hydraulic conductivity using a tension infiltrometer. Soil Sci. Soc. Am. J. 55, 633–639.

Schaap, M.G., Bouten, W., 1996. Modelling water retention curves of sandy soils using neural networks. Water Resour. Res. 32, 3033–3040.

Schaap, M.G., Leij, F.J., van Genuchten, M.Th., 1998. Neural network analysis for hierarchical prediction of soil water retention and saturated hydraulic conductivity. Soil Sci. Am. J., in press.

Šimůnek, J., van Genuchten, M.Th., 1996. Estimating unsaturated soil hydraulic properties from tension-disc infiltrometer data by numerical inversion. Water Resour. Res. 32, 2683–2696.

Šimůnek, J., van Genuchten, M.Th., 1997. Parameter estimation of soil hydraulic properties from multiple tension disc infiltrometer data. Soil Sci. 162, 383–398.

Šimůnek, J., Šejna, M., van Genuchten, M.Th., 1996. The HYDRUS-2D software package for simulating water flow and solute transport in two-dimensional variably saturated media. Version 1.0. IGWMC-TPS-53, International Ground Water Modeling Center, Colorado School of Mines, Golden, CO.

Smettem, K.R.J., Clothier, B.E., 1989. Measuring unsaturated sorptivity and hydraulic conductivity using multiple disk permeameters. J. Soil Sci. 40, 563–568.

Smiles, D.E., Knight, J.H., Perroux, K.M., 1982. Absorption of water by soil: the effect of a surface crust. Soil Sci. Soc. Am. J. 46, 476–481.

Tamari, S., Wösten, J.H.M., Ruiz-Suárez, J.C., 1996. Testing an artificial neural network for predicting soil hydraulic conductivity. Soil Sci. Soc. Am. J. 60, 1732–1741.

Thony, J.-L., Vachaud, G., Clothier, B.E., Angulo-Jaramillo, R., 1991. Field measurement of the hydraulic properties of soil. Soil Technol. 4, 11–123.

Tietje, O., Hennings, V., 1996. Accuracy of the saturated hydraulic conductivity prediction by pedo-transfer functions compared to the variability within FAO textural classes. Geoderma 69, 71–84.

Tietje, O., Tapkenhinrichs, M., 1993. Evaluation of pedotransfer functions. Soil Sci. Soc. Am. J. 57, 1088–1095.

Toorman, A.F., Wierenga, P.J., Hills, R.G., 1992. Parameter estimation of hydraulic properties from one-step outflow data. Water Resour. Res. 28, 3021–3028.

Valentin, C., Bresson, L.-M., 1992. Morphology, genesis and classification of surface crusts in loamy and sandy soils. Geoderma 55, 225–245.

van Genuchten, M.Th., 1980. A closed-form equation for predicting the hydraulic conductivity of unsaturated soils. Soil Sci. Soc. Am. J. 44, 892–898.

van Genuchten, M.Th., 1981. Non-equilibrium transport parameters from miscible displacement experiments. Research Report No. 119. U.S. Salinity Laboratory, USDA, ARS, Riverside, CA.

van Genuchten, M.Th., Leij, F.J., Yates, S.R., 1991. The RETC code for quantifying the hydraulic functions of unsaturated soils. EPA/600/2-91-065, U.S. EPA, Office of Research and Development, Washington, DC.

Vandervaere, J.-P., Peugeot, C., Vauclin, M., Angulo-Jaramillo, R., Lebel, T., 1997. Estimating hydraulic conductivity of crusted soils using disc infiltrometers and minitensiometers. J. Hydrol. 188–189, 203–223.

Warrick, A.W., 1992. Model for disc infiltrometers. Water Resour. Res. 28, 1319–1327.

White, I., Sully, M.J., 1987. Macroscopic and microscopic capillary length and time scales from field infiltration. Water Resour. Res. 23, 1514–1522.

Williams, R.D., Ahuja, L.R., Naney, J.W., 1992. Comparison of methods to estimate soil water characteristics from limited texture, bulk density, and limited data. Soil Sci. 153, 172–184.

Wooding, R.A., 1968. Steady infiltration from a shallow circular pond. Water Resour. Res. 4, 1259–1273.